RSC Advances




ROYAL SOCIETY OF CHEMISTRY

www.rsc.org/advances

RSC Advances

PAPER

# A core-shell CdTe quantum dots molecularly imprinted polymer for recognizing and detecting p-nitrophenol based on computer simulation

Yingchun Wang,[a] Ningwei Wang,[d] Xiaoni Ni,[b] Qianqian Jiang,[a] Wenming Yang,[c] Weihong Huang*[a] and Wanzhen Xu*[a]

In this study, the molecularly imprinted technology, which combined with fluorescence measure and the computer simulation, was used to detect contaminant p-nitrophenol. Using seven molecular dynamics simulations of molecular imprinting prepolymerization systems had been preformed to optimize the imprinting shell. Results indicated that the system with a p-nitrophenol (4-NP): 3-aminopropyltriethoxysilane (APTES): tetraethylorthosilicate (TEOS) mole ratio of 8 : 8 : 12 had the best stable template–functional monomer clusters. And the hybrid $SiO_2$ layer with CdS-like clusters on the surface of CdTe was synthesized by a simple reflux procedure. After that, the prepared imprinted materials (CdTe@$SiO_2$-MIPs) on the surface of silica contained CdTe nano particles (CdTe@$SiO_2$) by a surface imprinting and Stöber method polymerization were characterized by transmission electron microscopy, fluorescence spectroscopy, fourier transform infrared spectroscopy, ultraviolet visible analyzer, X-ray diffraction. A linear relationship between relative fluorescence intensity and the concentration of 4-NP had been obtained with a limit of detection of 0.08 μ mol/L and the imprinting factor (IF) was 2.23 which indicated that the special binding sites with the binding property to p-nitrophenol were created on the surface of the CdTe@$SiO_2$-MIPs materials. Ultimately, the feasibility of the fluorescent materials was successfully evaluated through the analysis of 4-NP in tap water and lake water. The recoveries were above 97.3%.

Received 00th January 20xx,
Accepted 00th January 20xx

DOI: 10.1039/x0xx00000x

www.rsc.org/advances

## 1 Introduction

Nitrophenols are classified as priority and persistent contaminants due to their relatively high toxicity, even at trace level concentrations in the aqueous matrices. Among the mono nitrophenols, p-nitrophenol (4-NP) which is regarded as a kind of intermediates[1] has been widely used to synthesize chemical drugs mainly in medicine, organic pesticide, fuel, etc. After using, these compounds are released into the environment and food chain through the effluents of various industries. Due to its genotoxicity and carcinogenesis,[2] it is a typical pollutant, and listed as one of 68 kinds priority control pollutants in China,[3] and one of the key control about 129 kinds of pollutants in Environmental Protection Agency.[4] It is toxic by inhalation or swallowing, contacting with skin that could result in dangerous of cumulative effects and high toxic to aquatic organisms. It can cause many different diseases such as dermatitis, methemoglobinemia and asthma, even lead to canceration and aggravate deterioration of tumor. Considering its harm come to us, the low concentration and high water solubility of 4-NP in the references water samples, the determination and re-concentration of 4-NP are very necessary in the further study. The conventional methods for 4-NP detection involve the chemical oxidation, colorimetric method, solvent extraction method and so on.[5-7] But in this regard, we synthesized fluorescent molecularly imprinted polymers (CdTe@$SiO_2$-MIPs) via the imprinting technology combined with fluorescence sensing and computer modeling was applied to recognize and detect 4-NP. Template 4-NP immobilizing was performed using 3-aminopropyltriethoxysilane (APTES) and tetraethoxysilicane (TEOS) to associate the target analyte on the surface of the fluorescent substrate CdTe QDs. According to molecularly dynamics simulation, the suitable ratio of

[a] School of Environment and Safety Engineering, Jiangsu University, Zhenjiang 212013, China. E-mail: whuang630@ujs.edu.cn xwz09@ujs.edu.cn Tel.: +86 511 88791919; fax: +86 511 88791947.
[b] Zhenjiang Institute for Drug Control of Jiangsu Province, Zhenjiang 212003, China.
[c] School of Material Science and Engineering, Jiangsu University, Zhenjiang 212013, China.
[d] Zhenjiang Entry-Exit Inspection Quarantine Bureau, Zhenjiang 212003, PR China.
† Electronic Supplementary Information (ESI) available: See
DOI: 10.1039/x0xx00000x

monomer/template was chosen. Then the ratio was applied to synthesize imprinting shell by imprinting technology.

Molecular imprinting is a process that functional monomers and cross-linking agents are copolymerized in the presence of the target analytes which act as molecular templates.[8-12] The target analytes or derivatives are employed as the templates to form complex with functional monomers via covalent or non-covalent interactions, such as hydrogen bonds, ionic and/or hydrophobic interactions, around that cross-linking monomers are arranged and co-polymerized to form a rigid polymer. The target analytes are regarded as the guidance to offer specific binding sites in the process of form molecularly imprinted polymers. After removal of the template, these tailor-made polymer materials would possess of special shape, size, binding sites, and then will exhibit a great affinity for template molecules.[13] In recent years, owning to many remarkable advantages such as structurally related compounds, high selectivity, physiochemical stability, low cost, specific recognition against the imprinted molecules[14] and easy preparation, molecularly imprinted polymers (MIPs) have been widely used to many fields like chromatographic separation, antibody mimetic, artificial receptor and catalysis.[15-19] But many challenges still remain to be addressed. One is the low yield of high affinity sites in the process of formation molecularly imprinted layer.[20,21] There are many studies aimed at improving the yield of high affinity binding sites including the stoichiometric imprinting strategy,[21,22] covalent imprinting mechanisms,[23] functional monomer dimerization[20] and site-selective chemical modification of molecularly imprinted polymers covalent imprinting mechanisms.[24] As a result, the excess functional monomers, which offer more background sites, are often added to ensure the formation of the most stable template-functional monomer clusters so that they can rise the affinity and selectivity for the guest molecules. Or empirical optimization via additional synthetic steps is the common approaches to synthesize the better MIPs. These methods are not rigorous and time-consuming. Computational chemistry, which can be designed the prepolymerization systems to choose the suitable ratio of templates and functional monomers, has been introduced in MIPs to avoid a functional monomer overdose and time-consuming.[25]

To further improve the selectivity and sensibility of MIPs, fluorescence is a meaningful signalling element because of its simplicity and low detection limit. Quantum dots (QDs), which are a kind of new-fashioned, highly luminescent semiconductor fluorescence (FL) material, have become of meeting with great favour due to their unique optical properties such as high quantum yield, narrow and symmetrical spectra, broad excitation spectra and photostability.[26, 27] Recently as their special traits, QDs have been a novel probe and combined with molecular imprinting technique in experiments. Many researchers have produced several kinds of fluorescence probes such as ZnS : $Mn^{2+}$ Quantum Dots,[28] CdSe,[29] CdZnTe alloyed quantum dots.[30] Nevertheless high stability is necessary for some highly sensitive detection. There have been some reports on coating $SiO_2$ layer on the surface of semiconductor materials.[37-38] For example, QDs which are introduced in various bio-application are coated with a thin shell.[36] However the formation of a $SiO_2$ shell with these means dramatically makes the fluorescence intensity reduce.[39] In the reference work,[40,41] CdTe@$SiO_2$ was prepared using a Stöber method by adding TEOS directly into the mixture of NaHTe, $Cd^{2+}$, mercaptopropanoic acid, meanwhile the silica shell was formed on the surface. This method is not conducive to form good core-shell structure and is effortless to cause problems or difficulties for FL detection. In this study, the modified sol–gel method with a certain time of backflow successfully made QDs cover with a thin hybrid $SiO_2$ shell. The hybrid $SiO_2$-coated CdTe was synthesized to achieve good core-shell structure and improve the problem that the fluorescence seriously decreased when the quantum dots were coated with $SiO_2$. The high FL efficiency was retained and the stability was increased as the CdS-like clusters embedded in $SiO_2$ shell on the surface of QDs (hybrid $SiO_2$-coated CdTe). And with the protection of the hybrid $SiO_2$ shell, their fluorescence lifetime was longer than that of the initial CdTe materials. Thus QDs coated with a hybrid $SiO_2$ shell should be a good candidate for supersensitive applications due to their extremely high FL efficiency and good stability in solution.

The hybrid $SiO_2$-coated QDs and computer simulation as auxiliary means in molecular imprinting technique were applied to detect 4-NP. The thioglycollic acid (TGA) functional CdTe QDs were synthesized in aqueous phase, and the modified sol-gel method with a simple a reflux process was used to coat with a thin hybrid shell CdS-like clusters on the surface of CdTe QDs. Molecular dynamics simulations were employed to optimize the imprinting shell of the fluorescent sensor and the employment of the hybrid $SiO_2$-coated CdTe with increasing FL efficiency. Simulation of molecular structure on computer as a kind of tools was applied to depict the three dimensional structure to help us more easily understand the molecule group members and the function of some special factions. The prepolymerizaiton systems were formed by 4-NP, APTES, TEOS and ethyl alcohol through the computer simulation. And the binding energy between special atoms in the systems was calculated by computer. Then according to the data concerning the intermolecular forces between molecules, the optimal molar ratio of the template/monomer was selected to synthesize MIPs. Furthermore, comparing with other methods, this way which only need to calculate the binding forces between molecules with the computer is much rapid, simple, convenient and low cost.

## 2. Results and discussion

### 2.1 The characterizations of CdTe QDs and CdTe@$SiO_2$

To investigate the effects of refluxing time on the optical properties of CdTe QDs, fluorescence spectrum of the CdTe QDs were monitored during the experiments. We could change the refluxing time to get different wavelength QDs. The results are presented in Fig. 1 (A, B). Beyond doubt, the refluxing time was not the only reason which could affect the QDs. One of other reasons was pH of the reactive solution before added the fresh precursor. In our experiments we chose pH=11.5, pH=12.0, pH=12.5 and pH=12.7 as comparisons. According to the results of Fig. 1 (A, B), these mixtures were refluxed for three hours, the fluorescence (FL) intensity results were presented as the Fig. 1 C. The factors which affect the QDs have many different aspects like temperature, refluxing time, pH, the quantity of the stabilizer and so on that would appeared in the experiments.[32] In this study, we just discussed time and pH, because these reasons cause relatively obvious changes of QDs.



 

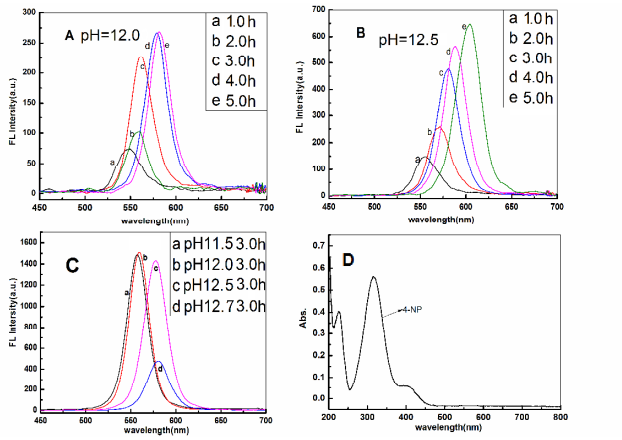


Fig. 1 FL spectra (A–C) of the thiol-capped CdTe QDs synthesized at 105℃. A is the FL Intersity of CdTe under pH=12.0 but different response time with PMT 500 and B is pH=12.5 with PMT 550. C is FL Intersity of CdTe with the same reaction time but different pH with PMT 700. D is the UV-Vis absorption spectroscopy of 4-NP.

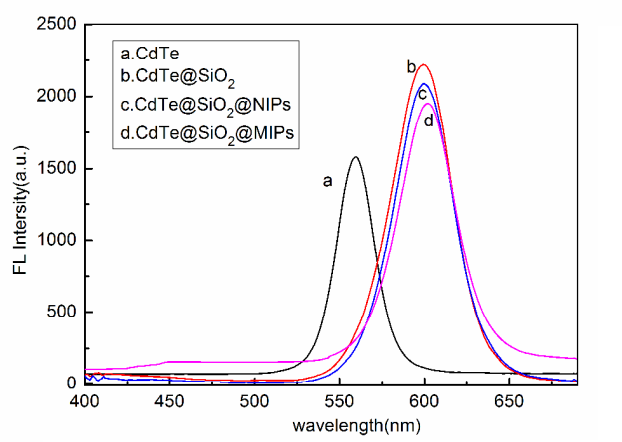


Fig. 2 FL spectra of the materials

Fig. 1 shows the FL emission behaviors of the CdTe QDs capped by TGA. As Fig. 1 (A, B), in general, the refluxing time process leads to a gradual increase in wavelength within the whole wavelength range of CdTe QDs and progressive red shifts at the wavelength onset. Accompanying with these variations in wavelength, fluorescence intensity is greatly enhanced as a function of the refluxing time in five hours. As the fluorescence intensity and wavelength increase gently after three hours, the CdTe QDs which were obtained on the three hours of refluxing time were chosen for the following preparation of the CdTe@$SiO_2$ composite particles. In Fig. 1 C, increasing tendency followed by decreasing is observed against pH for the FL emission of the CdTe QDs. The same refluxing time with different pH, fluorescence spectra are different. And it is obvious that the FL intensity of pH=12.0 is much better than others. So three hours refluxing time and pH=12.0 were chose for the following experiments. And considering the ultraviolet absorption peak of 4-NP in Fig. 1 D and preventing the occurrence of multiple frequency peak, the wavelength of QDs at 560 nm, which was the pH=12.0 and three hours refluxing time, was permissible.

As multicore or mononuclear CdTe@$SiO_2$ particles were obtained upon the use of prepared CdTe QDs, the modified sol-gel method was used to synthesize the hybrid $SiO_2$-coated CdTe. The seed-growth method, which was modified of the sol-gel method, could make the peak of QDs red shift, and the FL intensity could be increased as Fig. 2. During reflux, the CdS-like clusters nucleated and grew into the thin layer. The factor for the increased fluorescence efficiency should be the absence of an interface between the QDs and the generated clusters. The red shift is ascribed to a reduction of quantum size effect through the formation of CdS clusters in the vicinity of the QDs.

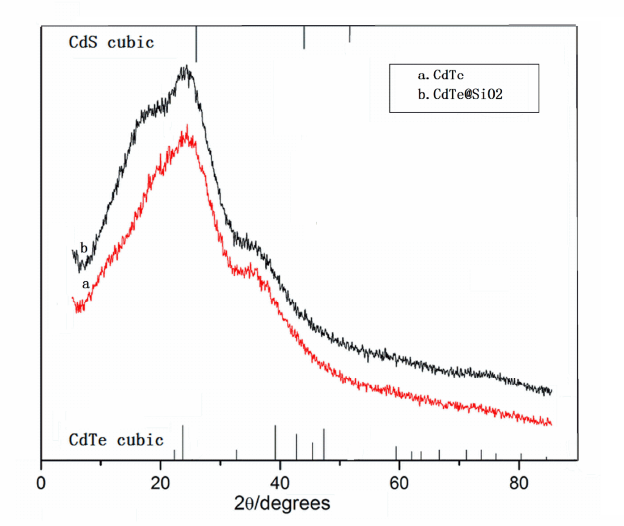


Fig. 3 XRD patterns of CdTe QDs (a) and CdTe@$SiO_2$ (b)

In the alkaline environment, the QDs were coated with a $SiO_2$ layer because of the partly hydrolysis of TEOS. Refluxing thirty minutes was introduced for the purpose of growing a hybrid $SiO_2$ shell on the QDs. A very thin silica layer was successfully integrated into the surface of the QDs in an alkaline CdTe colloidal solution with TGA and $Cd^{2+}$. The crystal structure formation and corresponding core/shell heterostructures of CdTe quantum dots were characterized by X-ray investigation. Fig. 3 displays the XRD pattern of CdTe and corresponding CdTe@$SiO_2$ nanoparticles. Fig. 3 a shows that as prepared TGA capped CdTe dots consists of the characteristics cubic Zinc blende CdTe pattern with diffractive peaks at 23.7°, 39.2° and 47.3°, which is also the dominant crystal phase of bulk CdTe, corresponding to (111), (220) and (311) planes of the reported CdTe peaks (JCPDS card no. 15-0770). And Fig. 3 b shows the hybrid $SiO_2$ shell including CdS-like clusters on the surface of CdTe QDs. At 2θ values of 20.7°, there appeared a peak in CdTe@$SiO_2$ particles, which can be indexed to $SiO_2$ spheres. And there are obvious shift from CdTe to CdS structure and the three distinct diffractive peaks of CdTe QDs weaken, these due to the existence the thin silica layer CdS-like clusters.

## 2.2 Computer simulation the prepolymerization of the CdTe@$SiO_2$-MIPs

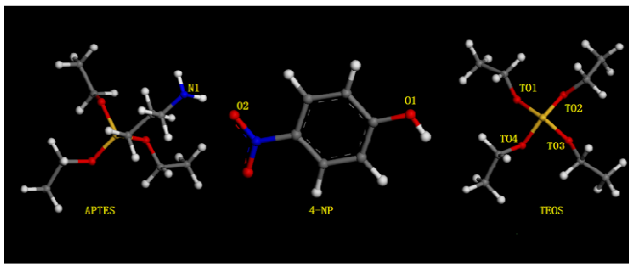


Fig. 4. The structures of 4-NP, APTES, TEOS and some binding sites

Table1 Composition of simulated MIP prepolymerization mixtures

| Type | 4-NP | APTES | TEOS | Solvent |
|---|---|---|---|---|
| APTES-MIP-1 | 8 | 10 | 32 | 100 |
| APTES-MIP-2 | 8 | 10 | 8 | 100 |
| APTES-MIP-3 | 8 | 10 | 16 | 100 |
| APTES-MIP-4 | 8 | 12 | 16 | 100 |
| APTES-MIP-5 | 8 | 8 | 10 | 100 |
| APTES-MIP-6 | 8 | 8 | 12 | 100 |
| APTES-MIP-7 | 8 | 8 | 16 | 100 |

The selectivity and sensitivity of the hybrid $SiO_2$-coated CdTe fluorescent sensor is endowed by the molecular imprinting shell. Hence it is of great importance for the analytical application of the fluorescent sensor that designing the imprinting shell possesses the optimal performance. The dummy computer molecular polymerization technology was used to preprepare the MIPs.[33] The ingredients of these prepolymerization systems are summarized in Table 1. Chemical structures and unique atom identifiers for molecules in molecular dynamics simulations were shown in Fig. 4. A comprehensive theoretical analysis of the interactions existing in the prepolymerization solution was undertaken, then results were applied to design the optimal quantitative relation of templates, functional monomers and cross-linking agents. The interactions between the amino (N1) of APTES and the hydroxyl (O1) and nitro (O2) of 4-NP were mainly analyzed. The radial distribution functions (RDFs) of these atoms which might form molecularly imprinted binding sites were shown in Fig. 5 and Fig. S1. Comparing Fig. S1 and Fig. 5, we could find that their maximum peaks were all around 3.0 Å but the degree of concentration of their peaks visible difference, especially for the interaction between O2 and N1. According to G. D.Olsson[42] depict, a bond cut off distance of 3.0 Å was used to analyze hydrogen bonding interactions. Therefore, all RDFs were integrated between 0.0 and 3.0 Å to calculate the average number of O within a spherical radius of 3.0 Å around N1. Fig 5 and Fig. S1 are RDFs showing the density of O around N during computer simulation. The one with lager radial shell number implies the greater density of O1 around N (O1-N1). And the density of O2 around N (O2-N1) which is regarded as the reference is shown in inset. Compared to O2-N1, the greater degree of N interaction with O1 is observed during all systems. So the focus of the following discussions lies in the interaction between O1 and N1.

As a comparison, APTES-MIP-1, APTES-MIP-2 and APTES-MIP-3 were selected to investigate the effect of concentration of cross-linking agents on the templates and functional monomers complexation. RDFs in Fig. S1 (A, B) of APTES-MIP-1 and APTES-MIP-2 show a relatively poorer interaction between O1 and N1 than interaction of APTES-MIP-3 in Fig. 5 A, most probably due to the quality of TEOS too much or too little. Too much would hinder APTES to move freely, on the contrary, that made APTES own enough large room so that 4-NP could not capture APTES. Then the peaks of the RFDs are not central at 3.0 Å. But APTES-MIP-3 shows a preferably radial distribution function. In this comparison, the prepolymerization mixtures of APTES-MIP-3 and the ratio of templates, functional monomers and cross linking agents are much better. Based on the result, fixing the ratio of templates and cross linking agents, we chose the APTES-MIP-3, APTES-MIP-4 and APTES-MIP-7 as another group of contrasts to optimize the concentration of functional monomers. The RDFs in Fig. 5 (A, B, D) show their interaction between O1 and N1. It is obvious that increasing the amount of APTES could not enhance the interaction between APTES and 4-NP. However, when the ratio of 4-NP and APTES was 8:8 as APTES-MIP-7, there is better result than others. The first possibility was that the higher concentration of cross-linking agents made APTES trap into the influence of space steric effect. So according to the comparison of these two groups, in order to get the optimum proportion of these mixtures, we did further comparison among APTES-MIP-5, APTES-MIP-6 and APTES-MIP-7. When the ratio of 4-NP and APTES was 8:8, no matter the amount of TEOS increased or decreased, the acting force of the binding sites could be little affected. What caused this phenomenon might be the self-assembly of APTES under the lower concentration cross-linker and the higher concentration of the cross-linking agent stopped the monomer closing to the template. But the RDFs of APTES-MIP-5 (6, 7) in Fig. S1 C and Fig. 5 (C D) show that the interaction between O1 and N1 of APTES-MIP-6 is a better uniform distribution around 3.0 Å. It is found that the optimal result is obtained when the ratio of 4-NP, APTES and TEOS was 8: 8:12 as shown in Fig. 5 C APTES-MIP-6. The interactions between O1 and N1, which the sharp and high peaks are around 2.85 Å, had transpired the formation of covalent bond. However, in order to prove the correctness of the results, we chose four prepolymerization mixtures that were APTES-MIP-3, APTES-MIP-4, APTES-MIP-6, APTES-MIP-7 as a contrast experiment to synthesize four groups CdTe@$SiO_2$-MIPs with the same method but different ratios.

RSC Advances

PAPER

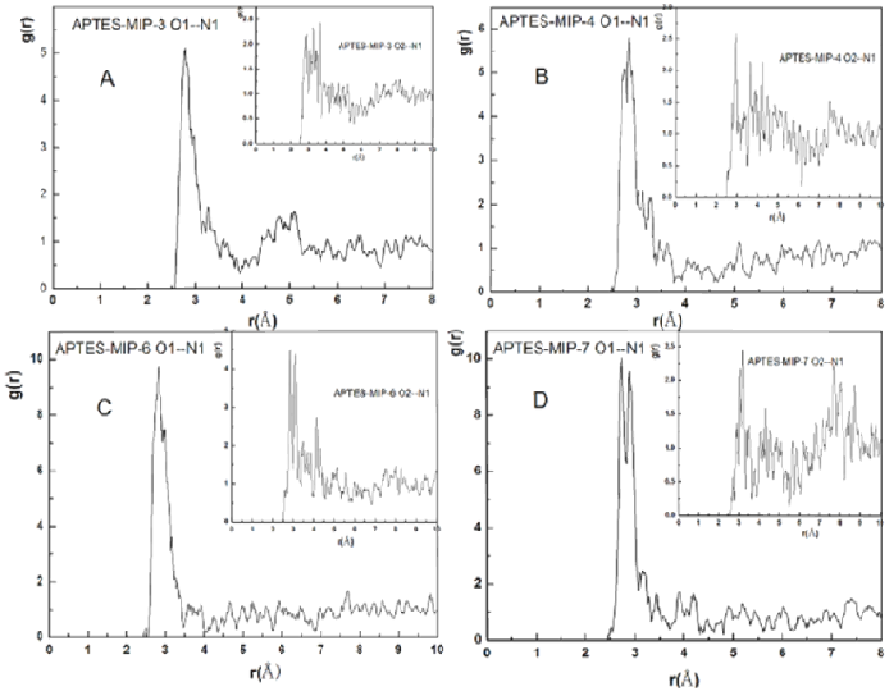


Fig. 5. RDFs showing the densities of APTES at different separation distances from the 4-NP functional groups in the prepolymerization mixtures when the ratios between 4-NP, APTES and TEOS change

### 2.3 Experimental verification of the simulation results

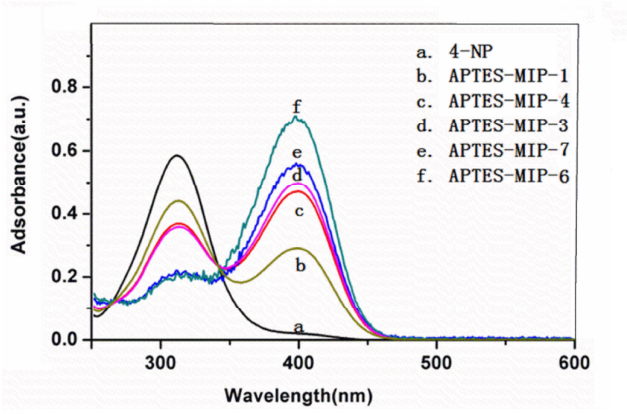


Fig. 6 Ultraviolet-visible spectra of different prepolymerization systems

In order to assure the reliability of the information, we did the ultraviolet absorption experiments by changing the proportion of mixtures according to the prepolymerization systems in the table 1. Based on the RFDs of these mixtures in Fig. 5 and Fig. S1, we chose five groups as a comparison. The reactive conditions were kept same with the synthesis of the CdTe@$SiO_2$-MIPs. It should be noticed that the hybrid $SiO_2$-cated CdTe QDs should not be added in these reactions. The results were shown in the Fig. 6. It is distinctly difference that the same concentration of 4-NP are added into the different quantities of the APTES and TEOS in the same solvent. And the absorption peaks of 4-NP at 315nm and 405nm have obviously changed in Fig. 6, they can certify the function between 4-NP and APTES. While the different quantities of APTES and TEOS affected the strength of the acting forces between the special atoms. There is the same phenomenon between APTES and TEOS, no matter increasing or decreasing of concentration would reduce the force. The suitable concentrations of these substances were very important. In the section the reactive system which was added as the prepolymerization mixture APTES-MIP-6 exhibited the better consequence which was consistent with the molecular dynamics simulations.

For further validation, CdTe@$SiO_2$-MIPs were synthesized by Stöber method. The structures and morphological characteristics of the resulting MIPs materials were detected by transmission electron microscope (TEM) as shown in Fig. 7. The products are core-shell particles, but it is not all products that can be clearly

observed the hybrid $SiO_2$-coated CdTe core and imprinting layer on the particles. As these can not be clearly observed, Fig. 7 (A, B) show a relatively poor image of APTES-MIP-3 and APTES-MIP-4 that are prepared with the ratios appearing in the table 1, these results correspond to RDFs in the Fig. 5 (A, B). Fig. 7 (C, D) show a relatively well image of APTES-MIP-6 that is synthesized with the ratio appearing in the table 1 and is corresponding to RDF in the Fig. 5 C. The shape of the APTES-MIP-6 was close to spherical with size in the range of 50.0±3.0 nm after coating with silica and the obtained hybrid $SiO_2$-coated CdTe core is about 5.0 nm in size. The hybrid $SiO_2$-coated CdTe core and imprinting layer on the every particle can be clearly observed. Fig. 7 E and F show better images of APTES-MIP-7 than A and B, but worse than C and D. The dispersity of the APTES-MIP-6 in the solvent and the dispersion degree of quantum dots in the imprinted layer was better than the others obviously. This result certified to the correctness of the molecular dynamics simulations again.

Comparing the TEM images and the ultraviolet absorption experiments which corresponded to computer simulation, we could also find that the ratio of synthesis APTES-MIP-6 was better. Therefore the all following experiments were accomplished with the ratio of APTES-MIP-6 to synthesize CdTe@$SiO_2$-MIPs. And the CdTe@$SiO_2$-NIPs were synthesized by the same method but without templates 4-NP.

## 2.4 Characterization of CdTe@$SiO_2$-MIPs and CdTe@$SiO_2$-NIPs

### 2.4.1 Fluorescence and infrared spectrum anslysis

The TEM analysis had done in the 2.3 section. And the images were shown in the Fig. 7.

The FL characters of the CdTe@$SiO_2$-MIPs and CdTe@$SiO_2$-NIPs were put in Fig. 2. Fig. 2 shows that the FL intensity of the CdTe@$SiO_2$-MIPs and CdTe@$SiO_2$-NIPs are lower than CdTe@$SiO_2$ and the peaks position have little shift, most probably because of much thickness of the layer and the large electric filed should be responsible for these phenomenon. Another may due to energy loss of the CdTe QDs when synthesizing the MIPs might have little duty for this phenomenon.

To ensure the successfully compound CdTe@$SiO_2$-MIPs on the surface of the CdTe@$SiO_2$, the FT-IR spectra of CdTe@$SiO_2$-MIPs, CdTe@$SiO_2$-NIPs and CdTe@$SiO_2$-4-NP are detected with the KBr disks and are compared in Fig. 8. As $SiO_2$ appeared in the above three materials, the peaks of the Si-O-Si and the Si-O which respectively were 1103 $cm^{-1}$ and 791 $cm^{-1}$ could be seen in all the spectra. According to a reference,[33] peak of N-H would be around 1500 to 1900 $cm^{-1}$ when the bending vibration took place. So we thought peaks of 1589 and 1556 $cm^{-1}$ in the spectrum of CdTe@$SiO_2$-4-NP（a）, CdTe@$SiO_2$-NIPs（b）and CdTe@$SiO_2$-MIPs （c）were the N-H of 4-NP and N-H of APTES, respectively. The peaks in the Fig. 8 (a) disappeared in the CdTe@$SiO_2$-MIPs (b) or only little. The N-H band around 1556 $cm^{-1}$ in Fig. 8 (a，b), resulting from APTES, proved successful synthesis CdTe@$SiO_2$-MIPs and CdTe@$SiO_2$-NIPs on the surface of the CdTe@$SiO_2$. The peaks at 1495 $cm^{-1}$, 1390 $cm^{-1}$, 856 $cm^{-1}$ and 642 $cm^{-1}$ were the bands C=C, O=N=O, C-N and C-H of CdTe@$SiO_2$-4-NP. These peaks missed in CdTe@$SiO_2$-MIPs to prove the imprinted sites existing. And the other aspects that the spectra of CdTe@$SiO_2$-MIPs and CdTe@$SiO_2$-NIPs were same also can prove the successful synthesis.

### 2.4.2 Stability of CdTe@$SiO_2$-MIPs

The stability of CdTe@$SiO_2$-MIPs was detected in water at room temperature shown in Fig. 9. The fluorescence intensity of CdTe@$SiO_2$-MIPs at twenty minutes is a little weak, but after thirty minutes the intensity increase a bit and remains stable in 70 minutes. The intensity was stable, as confirmed by the observed 3.9% RSD (relative standard deviation) for 12 replicate measurements of the solution of 30.0 mg $L^{-1}$ CdTe@$SiO_2$-MIPs materials within 70 minutes, mainly due to the inner location of the CdS-like clusters surrounded by the amorphous silica shell and partly due to the solution being ultrasonicated. The widths and the emission wavelength of the spectra remained the same. The phenomenon manifested that the silica layer was benefit to the stability of the material, as the silica shell compounded was necessary.

## 2.5 Characterization of analytical performance

### 2.5.1 Detection of CdTe@$SiO_2$-MIPs for different concentrations of 4-NP

To prove CdTe@$SiO_2$-MIPs for the template 4-NP a relatively well selectivity, we did further experiment that was the fluorescence analysis. The fluorescence quenching when different concentrations of 4-NP were added into CdTe@$SiO_2$-MIPs solution followed the Stern–Volmer equation which was shown in Fig. 10 inset.

$$F_0/F=1+K_{SV}[Q]$$

In the quenching kinetics equation $F_0$ and F are the FL intensities of the CdTe@$SiO_2$-MIPs before and after adding the template, respectively. Ksv is the Stern-Volmer constant, [Q] is the concentration of quencher. In the Fig. 10 A, when the concentration range of 10 μ mol/L to 60 μ mol/L, the fitting equation has a noticeably linear relationship with a correlation coefficient of 0.99734 for CdTe@$SiO_2$-MIPs, which can explain that the synthesized imprinted materials had the good recognition function for the template 4-NP through the quench degree of the fluorescence intensity. The linear regression equation of CdTe@$SiO_2$-MIPs is $F_0/F=0.99055+0.031189\bullet C_{4\text{-}NP}$. The lower limit of quantitation is calculated by 3σ/K, which is founded to be 0.08μmol/L. Compared with the fluorescence sensor based on Mn-doped ZnS quantum dots,[35] the fluorescence senor provides a wide linear range and high selectivity in this paper. The phenomenon was to blame for the binding sites on the surface of the CdTe@$SiO_2$-MIPs, these sites made the template reunite with the CdTe@$SiO_2$-MIPs. In addition, the CdTe@$SiO_2$-NIPs materials have the same quenching phenomenon with a correlation coefficient of 0.99115. The IF was 2.23 in the Fig. 10. And the peaks position of CdTe@$SiO_2$-MIPs and CdTe@$SiO_2$-NIPs materials had been little affected as various amounts of 4-NP added. The non-covalent interactions between the specified atoms through electron transfer should be responsible for this phenomenon.

The results indicated when the template was added into the CdTe@$SiO_2$-MIPs materials, the FL intensity of the materials decreased obviously, so these materials had the better detection.



 

RSC Advances

PAPER

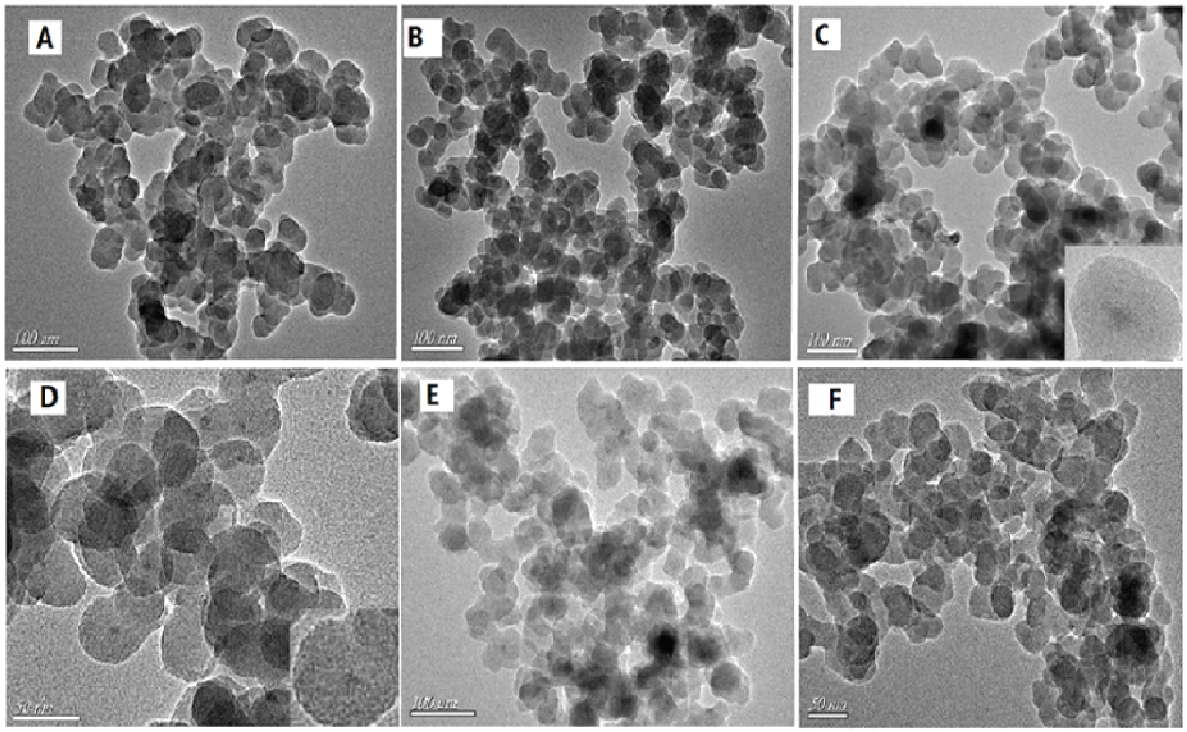


Fig. 7 TEM images of APTES-MIP-3 (A), APTES-MIP-4 (B), APTES-MIP-6 (C, D) and APTES-MIP-7 (E, F).

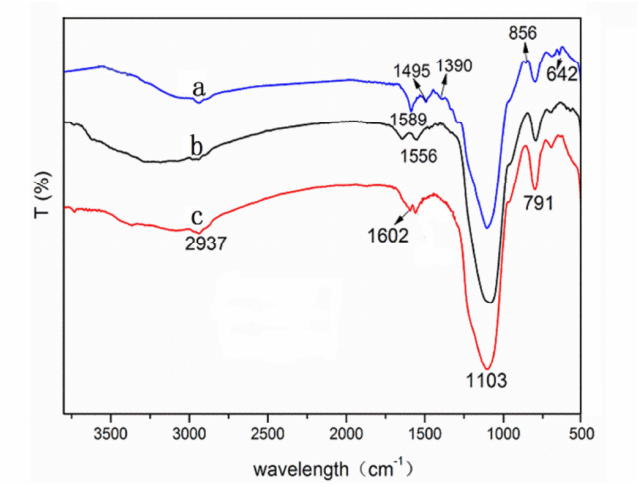


Fig.8 FT-IR spectra of the CdTe@$SiO_2$-4-NP (a), CdTe@$SiO_2$-NIPs (b), CdTe@$SiO_2$-MIPs (c).

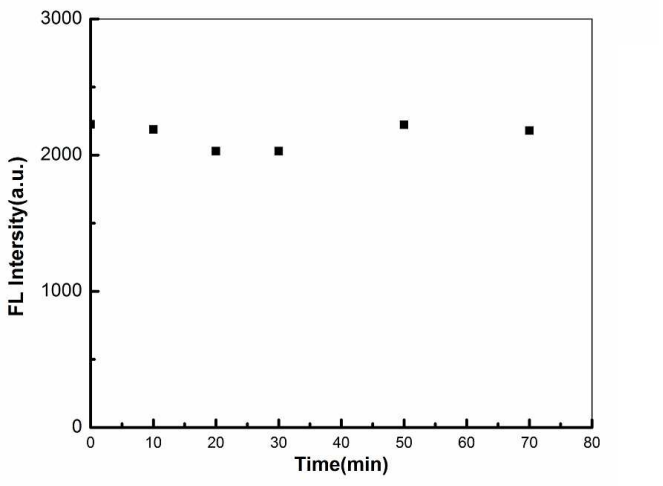


Fig.

9 The stability of the CdTe@$SiO_2$-MIPs at room temperature.

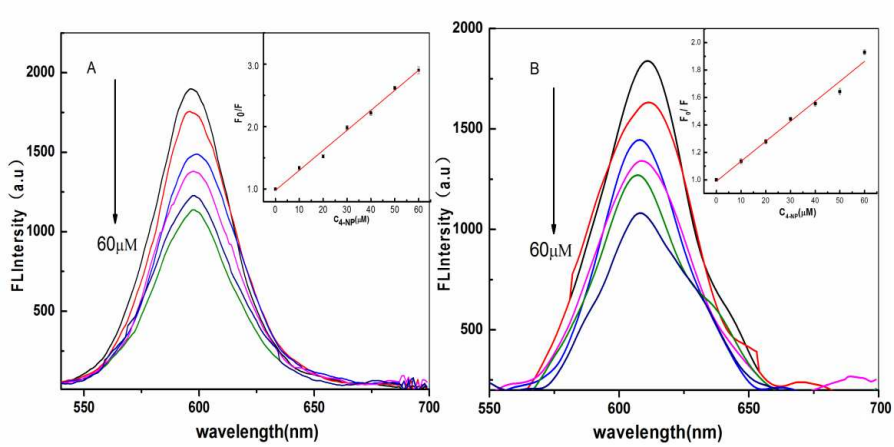


Fig.10 Fluorescence emission spectra of CdTe@$SiO_2$-MIPs （A）and CdTe@$SiO_2$-NIPs（B） at different concentrations of 4-NP in water solution and corresponding Stern–Volmer curve (inset).

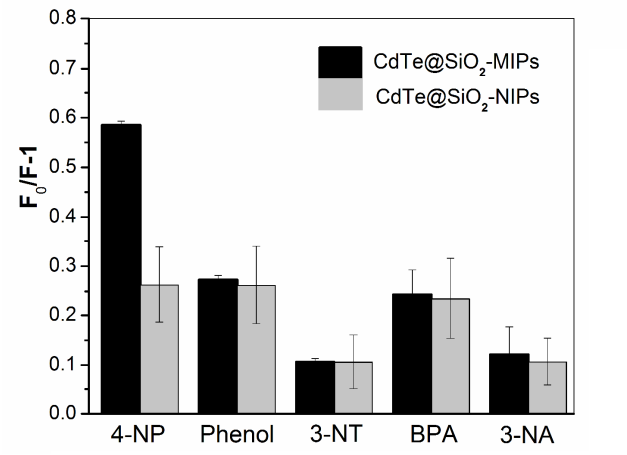


Fig.11 The selectivity of CdTe@$SiO_2$-MIPs and CdTe@$SiO_2$-NIPs

### 2.5.2 Selectivity adsorption of the CdTe@$SiO_2$-MIPs

To prove the better selectivity of CdTe@$SiO_2$-MIPs for 4-NP, we chose methylnitrobenzene (3-NT), nitrophenylamine (3-NA), phenol and bisphenol A (BPA) as the reference substances shown in Fig. 11. For 4-NP, the CdTe@$SiO_2$-MIPs exhibited much more selectively than the CdTe@$SiO_2$-NIPs and the other substances. The binding sites with respect to the template were synthesized in the process and the special recognition sites were grafted on the surface of the CdTe@$SiO_2$-MIPs, so 4-NP could easily reunite with CdTe@$SiO_2$-MIPs materials, then caused a certain degree of fluorescence quenching. As for the others, the imprinting sites were not matching with them, so they has little fluorescence quenching. Due to the interaction between hydroxyl and the amino, the selectivity of BPA and phenol was relatively better. But compared with 4-NP, their selectivity was weak. So the CdTe@$SiO_2$-MIPs materials had a good selectivity for 4-NP.

### 2.5.3 Application to water sample analysis

Table 2 Determination of 4-NP in the tap water and lake water (n=3)

| samples | spiked (μM) | found (μM) | recovery (%) | RSD (%) |
|---|---|---|---|---|
| tap water | 0.0 | 0.0 | | |
| tap water | 7.5 | 7.4 | 98.7 | 4.8 |
| tap water | 25.0 | 25.2 | 100.8 | 2.4 |
| tap water | 50.0 | 50.1 | 100.2 | 1.6 |
| lake water | 0.0 | 0.0 | | |
| lake water | 7.5 | 7.3 | 97.3 | 6.4 |
| lake water | 25.0 | 25.8 | 103.2 | 5.1 |
| lake water | 50.0 | 51.1 | 102.2 | 2.1 |

The practicability of the fluorescence senor CdTe@$SiO_2$-MIPs was evaluated by detecting 4-NP concentration in real water samples. According to the linear regression equation, three different concentrations of 4-NP were added into tap and lake water, respectively, and detected the recovery rate. The results were indicated as the table 2.

The recovery rates are between 97.3% and 103.2%, and the RSDs are relatively low. So the fluorescence senor in this work could be used to accurately measure 4-NP in the water environment.

## 3. Experimental section

### 3.1 Materials and reagents

Tellurium powder (Te), sodium borohydride ($NaBH_4$) and thioglycolic acid (TGA) were obainted from Aladdin. Cadmium chloride($CdCl_2 \cdot 2.5H_2O$), p-nitrophenol (4-NP), methylnitrobenzene

(3-NT), nitrophenylamine (3-NA), phenol, bisphenol A (BPA), sodium hydroxide (NaOH), ammonium hydroxide ($NH_3 \cdot H_2O$) were obtained from Shanghai Chemical Reagent Company (Shanghai, China). 3-aminopropyltriethoxysilane (APTES), and tetraethoxysilicane (TEOS) were obtained from Alfa Aesar. All chemistry drugs in our experiments are analytical grade. The aqueous solutions we have used are deionized water.

### 3.2 Characterization

Fluorescence (FL) measurements, UV–vis spectra (200–800 nm) were recorded on a UV-2450 spectrophotometer (Shimadzu). Using Nicolet NEXUS-470 FT-IR apparatus (USA) recorded Infrared spectra (4000–400 $cm^{-1}$) in KBr, transmission electron microscope (TEM, JEOL, JEM-2100) and the D8 Advance X-ray powder diffraction.

In the experiments, all fluorescence detections were performed under the same condition: the excitation wavelength was set at 365 nm. The slit widths (5nm) were kept constant within each data set. Apart from the PMT Voltage, it was different. 500V, 550V corresponded to Fig.1 A, Fig. 1 B, respectively. And the PMT Voltage of the other figures about FL intersity was 700V.

### 3.3 Synthesis of hydrosulfuryl modified CdTe QDs

CdTe QDs were synthesized in aqueous solution as the description in other documents[31] with little modification. We compounded aqueous CdTe QDs with thioglycolic acid as stabilizer, what we need before synthesizing CdTe QDs was fresh precursor sodium hydrogen telluride (NaHTe**).**

The fresh precursor NaHTe had been synthesized with 125.0 mg Tellurium powder (Te), 200.0 mg sodium borohydride ($NaBH_4$) and 10.0 mL deionization water. We added Te and $NaBH_4$ into a vitreous bottle which could accommodate 15.0 mL liquid probably, after that 10.0 mL deionization water was added. Next to put into ice-bath, contemporary stirring constantly until milky appeared.

In order to make better use of time, when the best precursor was on the road, we put 553.0 mg Cadmium chloride ($CdCl_2 \cdot 2.5H_2O$) and 284.0 mg thioglycolic acid (TGA) into 175.0 mL deionization water. The mixture was adjusted to pH=12.0 with 1 M NaOH, and strongly stirred under the protection of nitrogen for 30 min. Then 6.0 mL clear milky and fresh solution NaHTe was added to this mixture quickly, and reacted at 100℃ with stirring and refluxing for several hours. Stable aqueous solution of thioglycolic acid capped CdTe QDs were synthesized, then the CdTe that was placed seven days was used to next step.

### 3.4 Preparation of CdTe@$SiO_2$

We used the seed-growth method, the “seed” was the pure QDs which was prepared by the hydro-thermal method. To a 250 mL flask, 150.0 mL of a mixed water solution of 114.0 mg $CdCl_2 \cdot 2.5H_2O$ and 138.0 mg TGA, and this mixture was adjusted to pH=10.5 with 1 M NaOH, and subsequently 15.0 mL CdTe which was placed seven days was added into this flask, and then 7.5 mL $NH_3 \cdot H_2O$ (6.25wt%) and 2.0 mL TEOS were also added, then reacted 3 hours in the room temperature avoiding light. In the end the mixture solution was refluxed for 30 minutes to generate CdS-like clusters in the $SiO_2$ shell at 100℃.

### 3.5 Molecular dynamics simulations

The monomers that are extensively used are 4-vinylpyridine (4-VP), acrylamide (AM), methyl acrylic acid (MAA) and so on. But which one should be used, according to the acid-base properties and functional groups of these monomers. At the same time, the cross-linking also affects the characteristics of recognition of MIPs. During the research, we used APTES as the monomers, TEOS as the cross-linking agents because they are eco-friendly and they can not affect the surface stability of the CdTe QDs which was synthesized under alkaline conditions. The molecular structures of the template, APTES, TEOS were presented in Fig. 1, and some structures of molecules that may form typical binding sites were put into the table 1.

First using molecular dynamics, the molecular structures and the energy of the template 4-NP, APTES and TEOS were optimized before molecular simulation of the prepolymerization. What used was the Material Studio 7.0 Windows (Accelrys Inc., San Diego, CA92121, USA) software in the model. And all the optimized systems and the simulation procedures had done under the COMPASS force field. Then the systems of prepolymerization were built and optimized with the Construction order of the Amorphous cell. All the composition units we built were seven groups, the temperature kept at 298 K, and the density was stipulated at 1.3 g/mL. The seven group prepolymerization mixtures were optimized with the method just like the way that deal with the molecules. The primary procedures we used were the SMART MINIMIZER in the Discover Tools, the iterations were set at 20,000. These seven kinds of prepolymerization systems were built with the different mole ratios of materials as table 1.

Through the optimized procedure, these mixtures might be not stable. In order to avoid the bad situation occur, we finished the molecular dynamics simulation procedures of these prepolymerization systems after the SMART MINIMIZER. The simulation procedure not only could ensure the prepolymerization systems to be optimized stable, but also could make these systems balance relatively in the energy state. In the first place, we used the Dynamics order of the Discover module to adopt the NVT molecular dynamics system, the COMPASS force field in the opened Dynamics taskbar to make the prepolymerization system balance 200 ps at 298 K. The VDW and non-bonding interaction of Coulomb were used the atom-based and Ewald to calculate sums respectively. These summation methods had been made 200,000 steps to calculate. The Radial Distribution Function (RDF) was used to analyze the monomer distribution around the template with the change of the cross-linking.

### 3.6 Preparation of CdTe@$SiO_2$-MIPs and CdTe@$SiO_2$-NIPs

CdTe@$SiO_2$-MIPs were synthesis with Stöber method by using computer simulation to select the best molar ratio. In order to let computer simulation be more convincing, we did four groups experiments according to APTES-MIP-3, APTES-MIP-4, APTES-MIP-6, APTES-MIP-7 in table 1. They were synthesized with the same way

like APTES-MIP-6 only accepted different ratios. APTES-MIP-6 was synthesized with following steps. First 30.0 mg 4-NP dissolved into 20.0 mL ethyl alcohol, 15.0 mL CdTe@$SiO_2$ and 40.0 μL APTES were added in the mixture with vigorous stirring. After 30 min 70.0 μL TEOS as the cross-linking agent were mixed in the solution, and in order to make the mixture more speed reaction 100.0 μL $NH_3 \cdot H_2O$ (6.25 wt%) be added, then the reaction sustained 8 hours under room temperature. Then the product was washed with ethylalcohol several times, the supernatant was discarded, the nanometer materials were centrifuged at 6000 rpm for 10 min, and repeated several times until the template disappeared that was said the yellow substance missed. Then the materials were dried at 35 ℃ for 24 hours under a vacuum for further use.

As a comparison, the non-imprinted polymer materials (CdTe@$SiO_2$-NIPs) were synthesized with the same method but did not add template molecules.

### 3.7 FT-IR measurements

The samples which were used to measure must be dry, and the KBr were used as the auxiliary materials. These materials were measured including CdTe@$SiO_2$, CdTe@$SiO_2$-MIPs, CdTe@$SiO_2$-NIPs and the CdTe@$SiO_2$-MIPs with some template （CdTe@$SiO_2$-4-NP）.

### 3.8 Fluorescence detection

In our experiments, fluorescence is one of the important tools to represent the effect. All fluorescence detections were under the same condition with the emission wavelength at 365 nm unless detected the selectivity and recognition of the CdTe@$SiO_2$-MIPs, and the examination area at 400 nm-700 nm.

Same amounts materials 10.0 mg which were pre-prepared CdTe@$SiO_2$-MIPs, CdTe@$SiO_2$@-NIPs and the materials CdTe@$SiO_2$-MIPs without washing the template 4-NP were dissolved in 100.0 mL deionization water and then concussed with ultrasonic until the solid disappeared. Then we scanned these substances at room temperature. At the same condition, alcohol solution dissolved different amounts of 4-NP to get different concentrations, such as 10.0, 20.0, 30.0, 40.0, 50.0, 60.0 μmol•$L^{-1}$ to dissolve respectively 5.0 mg CdTe@$SiO_2$-MIPs beads into 10.0 mL 4-NP solution stirring until the beads fade away. Last at the same condition the fluorescence intensity was detected.

### 3.9 Selectivity and recognition

In order to test the selectivity of the CdTe@$SiO_2$-MIPs to 4-NP, we chose 3-NT, 3-NA, phenol and BPA as the analogues. To make different concentrations of 4-NP, 3-NT, 3-NA, phenol and BPA solutions, we added the same amount of CdTe@$SiO_2$-MIPs, CdTe@$SiO_2$-NIPs into every kind solution one by one, and did the same procedure as the fluorescence measurement, which the excitation wavelength was at 315 nm. And then the date was recorded at 605 nm, in other words the fluorescence intensity of 605 nm was recorded at room temperature.

### 3.10 Analysis of tap water and lake water

Water samples pretreatment were based on the means to pretreat by Chunxiao Qiu.[34] Typically, the lake water was gathered from the Yudai River in Jiangsu University, and the tap water was collected from the water in the lab. This experiment adopted the method of standard addition recovery, and prepared 7.5, 25.0, 50.0 μmol•$L^{-1}$ solutions of the template, respectively.

## 4. Conclusions

A novel route to obtain the fluorescent molecularly imprinted polymer materials CdTe@$SiO_2$-MIPs, which combined with computer simulation, had been presented in this work. First, the fluorescent CdTe QDs were successfully coated with a layer of hybrid $SiO_2$ to fortify the stability and FL intensity of hydrosulfuryl modified CdTe QDs. Then by a series of comprehensive molecular dynamics studies, the optimal proportion 8:8:12 of 4-NP, APTES and TEOS was chose and the result was verified by the ultraviolet absorption experiments and TEM studies. The characteristic analysis of CdTe@$SiO_2$-MIPs had indicated that the dispersion of CdTe quantum dots in CdTe@$SiO_2$-MIPs showed a good selectivity and sensitivity. The real samples detection revealed that this method was feasible and the materials had a good performance to detect 4-NP.

## Acknowledgements

This work was financially supported by the Jiangsu Natural Science Foundation of China (No. BK20141287). This work was partly financially supported by the Senior Talent Foundation of Jiangsu University (No. 14JDG057), Postdoctoral Science Foundation of China (No.2014M560405, 2015T80515), Postdoctoral Science Foundation of Jiangsu Province (No. 1401012A), Zhenjiang Social Development Fund of Jiangsu Province (No. SH2014020), the Scientific Research Foundation of Jiangsu University (No. 13A581).

## References

1 H. Hmitt , R. Altenburger , B. Jastorff , G. Schuurmann. Chemical Research in Toxicology, 2000, **13**, 441.

2 G. Eichenbaum, M. Johnson, D. Kirkland, P. O'Neill, S. Stellar, J. Bielawne, R. DeWire, D. Areia, S. Bryant, S. Weiner, D. Desai-Krieger, P. Guzzie-Peck , D. C. Evans, A. Tonelli. Regulatory Toxicology and Pharmacology, 2009, **55**, 33.

3 W. M. Zhou, D. Q. Fu, Z. G. Sun. Environmental Monitoring In China, 1990, **6**, 1.

4 USEPA (United States Environmental Protection Agency). Washington: Health and Ecological Criteria Division, 1991.

5 L. L. Wang, H. Yang, L. Zhang, X. H. Lu. Industrial Water Treatment, 2003, **23**, 23.

6 J. F. Pang, L. S. Wang, X. N. Fei, J. H. Zhang. Urban Environment & Urban Ecology, 2003, **16**, 34.

7 X. C. Zeng, L. X. Li. Environmental Engineering, 1990, **8**, 1.



 

8 Q. Huamin, X. Li, L. Li, S. Min, L. Chuannan. Carbohyd. Polym.,2013, **92**, 394.
9 Y. F. Du, X. H. Fang, W. J. Sun. Journal of AnHui Agricultural Sciences, 2012, **34**, 16507.
10 O. Ramström, J. A. Richard. Chirality, 1998, **10**, 195.
11 Z. Y. Jiang, Y. X. Yu, H. Wu. Membrane Science and Technology, 2006, **1**, 78.
12 L. X. Chen, S. F. Xu, J. H. Li. Chem. Soc. Rev., 2011, **40**, 2922.
13 X. L. Qi, Y. Q. Wang, S. Y. Zhang, S. Wei, A. P. Wei. Chemical Research and Application, 2009, **4**, 441.
14 F. Lanza, B. Sellergren. Chromatographia, 2001, **53**, 599.
15 P. Spégel, L. Schweitz, S. Nilsson. Anal. Bioanal.Chem., 2002, **372**, 37.
16 J. Q. Liu, S. C. Shen. Journal of Functional Polymers. 1998, **4**, 561.
17 K. Haupt, K. Mosbach. Chem. Rev., 2000, **100**, 495.
18 S. Farzaneh, E. Asadi, M. Abdouss, A. Barghi-Lish, S. Azodi-Deilami, H. A. Khonakdar and M. Gharghabi. RSC Adv., 2015, **5**, 9154.
19 Ana P. M. Tavares, Felismina T. C. Moreira, M. Goreti F. Sales. RSC Adv., 2013, **3**, 26210.
20 L. Ye, K. Haupt. Anal. Bioanal. Chem., 2004, **378**, 1887.
21 P. Manesiotis, A.G. Hall, M. Emgenbroich, M. Quaglia, E.D. Lorenzo, B. Sellergren, Chem. Commun. 2004, 20,2278.
22 A.J. Hall, P. Manesiotis, M. Emgenbroich, M. Quaglia, E.D. Lorenzi, P.J. Sellergren, J. Org. Chem. 2005,70,1732.
23 R.J. Umpleby, M. Bode, K.D. Shimizu. Analyst 2000,125, 1261.
24 R.J. Unpleby, G.T. Rushton, R.N. Shah, A.M. Rampey, J.C. Bradshaw, J.K. Berch, K.D.Shimizu. Macromolecules, 2001, 34, 8446.
25 L.K. Liu, Y. Cao, P.F. Ma, C.X. Qiu, W.Z. Xu, H. Liu, W.H. Huang. RSC Adv. 2014, 4, 605.
26 M. Bruchez, M. Jr. Moronne, P. Gin, S. Weiss, A. P. Alivisatos. Science, 2013, **281**.
27 Z. Y. Tang, N. A. Kotov, M. Giersig. Science, 2002, **297**, 237.
28 L. Tan, C. C. Kang, S. Y. Xu, Y. W. Tang. Biosensors and Bioelectronics, 2013, **48**, 216.
29 Y. Zhu, Z. Li, M. Chen, Helen M. Cooper, G. Q. Lu, Z. P. Xu. Journal of Colloid and Interface Science, 2013, **390**, 3.
30 J. W. Cheng, D. M. Li, T. Cheng, B. Ren, G. Wang, J. Li. Journal of Alloys and Compounds, 2014,**589**, 539.
31 L. Zhou, C. Gao, X. Z. Hu, W. J. Xu. ACS Appl. Mater. Interfaces, 2010, **4**, 1211.
32 X. M. Liu, J. T. Tian, J. H. Dai, X. Wang. Physica E, 2014, **57**, 56.
33 L. Z. Meng, S. L. Gong, Y. B. He. Wuhan University Press, 1997.
34 C. X. Qiu, Y. H. Xing, W. M. Yang, Z. P. Zhou, Y. C. Wang, H. Liu, W. Z. Xu. Applied Surface Science, 2015, **345**, 405.
35 H. F. Wang, Y. He, T. R. Ji. X. P. Yan. Anal. Chem., 2009, **81**, 1615.
36 A. Wolcott, D. Gerion, M. Visconte, J. Sun, A. Schwartzberg, S. Chen, J. Z. Zhang, J. Phys. Chem. B 2006, **110**, 5779.
37 T. Nann, P. Mulvaney. Angew. Chem., 2004, **43**, 5511.
38 V. Salgueirin˜o-Maceira, M. A. Correa-Duarte, M. Spasova, L. M. Liz-Marza´n, M. Farle. Adv. Funct. Mater., 2006, **16**, 509.
39 Y. Chan, J. P. Zimmer, M. Stroh, J. S. Steckel, R. K. Jain, M. G. Bawendi,. Adv. Mater., 2004, **16**, 2092.
40 Y. Zhu, Z. Li, M. Chen, H. M. Cooper, G. Q. Lu, Z. P. Xu. Journal of Colloid and Interface Science, 2013, **390**, 3.
41 L. Zhou, C. Gao, X. Z. Hu, W. J. Xu. ACS Applied Materials & Interfaces, 2010, **2**, 1211.
42 G. D.Olsson, B. C.G.Karlsson, E. Schillinger, B. Sellergren, I. A.Nicholls, Ind. Eng. Chem. Res. 2013, **52**, 13965.
43 H. B. Bao, Y. J.Gong, Z. Li, M. Y. Gao. Chem. Mater.2004,**16**, 3853.